

Crystal structures and electron densities of nickel and iron silicate spinels at elevated temperature or pressure

LARRY W. FINGER, ROBERT M. HAZEN AND TAKEHIKO YAGI¹

Geophysical Laboratory
Carnegie Institution of Washington
Washington, D. C. 20008

Abstract

The lattice parameters and crystal structures of the spinel form of Ni_2SiO_4 have been determined at various pressures using a miniature diamond pressure cell and, at one atmosphere, at elevated temperatures. The crystal structure of the spinel form of Fe_2SiO_4 has been refined from data measured under room conditions. All refinements have weighted residuals in the range 1.4 to 2.4 percent. The oxygen positional parameter, u , increases with higher pressure or lower temperature. The relationship between u and unit-cell edge, a , is essentially linear. The Si-O distance is approximately constant with a value of 1.66 Å for all temperatures, pressures, and compositions. Thus thermal expansion and compression of silicate spinel is mostly due to changes in the octahedral site. The polyhedral bulk modulus is 1.7 ± 0.1 Mbar for the Ni-O octahedron and is greater than 2.5 Mbar for the Si-O tetrahedron.

Modification of the temperature factor model to include anharmonic terms greatly reduces the residual electron density for Ni_2SiO_4 ; however, similar factors for Fe_2SiO_4 are not significant.

Introduction

The spinel form of magnesium-iron orthosilicate, $(\text{Mg,Fe})_2\text{SiO}_4$, is believed to be a major rock-forming mineral in the mantle (Ringwood, 1958a). An understanding of the crystal chemistry of silicate spinel, therefore, is important in defining the equation of state of the solid earth. The olivine/spinel phase transition (Ringwood, 1958b) is a reconstructive transformation that has been the subject of numerous experimental and theoretical studies (for a review, see Wyllie, 1970, p. 123-130).

The space group of silicate spinels is $Fd\bar{3}m$, $Z = 8$. For the standard origin at a center of symmetry, the three atoms in the asymmetric unit are R^{2+} at $(1/2, 1/2, 1/2)$, Si at $(1/8, 1/8, 1/8)$, and O at (u, u, u) with $u \approx 0.24$. Two parameters, the oxygen positional parameter u and the cubic cell edge a , are sufficient to define completely the crystal structure of a silicate spinel.

Both the olivine and the spinel forms of $R_2^+\text{SiO}_4$

have Si in tetrahedral coordination and R^{2+} in octahedral coordination. Kamb (1968) demonstrated that an important difference between these two structures is the type of edge-sharing between cation polyhedra. Unlike the olivine form, the spinel form has no edges shared between tetrahedra and octahedra. In the silicate spinels, furthermore, the edges shared between octahedra are longer than the unshared edges as a result of the oxygen positional parameter, u , being less than 1/4. All spinel structures stable at 1 bar have u greater than 1/4. Kamb further suggested that the ratio of octahedral to tetrahedral metal-oxygen bond instances, d_o/d_t , will be important in the stabilization of a given phase. If this ratio is greater than some critical value, the olivine structure is stabilized, whereas if it is less than that value, spinel is the stable form. Changes in temperature, pressure, or composition alter the bond-distance ratio. Syono *et al.* (1971) noted that crystal-field effects for transition-metal ions are an additional factor influencing the olivine/spinel transition.

To test the Kamb model it is necessary to determine the crystal structures of olivine and spinel under the conditions of transformation. The data for

¹ Present address: Institute for Solid State Physics, University of Tokyo, Roppongi, Minato-ku, Tokyo 106, Japan.

olivine at high temperature (Smyth, 1975; Smyth and Hazen, 1973) and at high pressure (Hazen, 1977) have been presented; however, analogous data for silicate spinels have not been reported.

The crystal structures of γ -Fe₂SiO₄ and γ -Ni₂SiO₄ were reported by Yagi *et al.* (1974), and γ -Co₂SiO₄ was described by Morimoto *et al.* (1974). These room-pressure studies of metastable single crystals yielded anomalously high Si-O distances (≈ 0.03 Å larger than in olivines) and short R²⁺-O distances (≈ 0.03 Å shorter than in olivines). Additional experiments by Marumo *et al.* (1974, 1977) revealed systematic residual electron densities near the positions of R²⁺ cations.

The principal objectives of this study are

- (1) to determine separately high-pressure structures and a high-temperature structure of γ -Ni₂SiO₄,
- (2) to compare olivine and spinel structures near conditions of transformation, and
- (3) to determine the cause of electron density residuals near the octahedral cation.

Experimental

Specimen description

Single crystals of synthetic iron and nickel silicate spinels were selected from material synthesized in a tetrahedral anvil high-pressure apparatus. The material was also used in previous room-condition refinements of the structures (Yagi *et al.*, 1974). The conditions of synthesis were 75 kbar and 1500°C for Fe₂SiO₄ and 55 kbar and 1400°C for Ni₂SiO₄.

The measurements of integrated intensities were performed with the computer-controlled, single-crystal diffractometer described by Finger *et al.* (1973). Molybdenum radiation ($\lambda = 0.70926$ Å) and a θ - 2θ scan technique were used, with the background counting time and scan rate adjusted to yield a constant ratio of the intensity to its standard deviation (σ_I) computed from counting statistics. Two standard reflections were remeasured every 2 hr to test for drift. For the measurements under room conditions, one octant of reciprocal space was measured to a maximum $\sin\theta/\lambda$ of 0.9 with a value of 0.01 for σ_I/I . At high temperature, one octant of reciprocal space was measured to a maximum $\sin\theta/\lambda$ of 0.75. The preferred value of σ_I/I was 0.02. At high pressures, the intensity measurements included all accessible reflections in a hemisphere of reciprocal space with $\sin\theta/\lambda$ less than 0.7. The preferred value of σ_I/I was

0.02, and all intensities were measured using the fixed- ϕ mode of data collection (Finger and King, 1978). All intensities were corrected for absorption by the diamond cell, if appropriate, and for absorption by the crystal ($\mu_i = 148.1$ cm⁻¹ for Ni₂SiO₄ and 106.3 cm⁻¹ for Fe₂SiO₄).

High-pressure techniques

One iron- and three nickel-silicate spinel single crystals approximately 70 × 70 × 50 μm were mounted in diamond-anvil pressure cells (Merrill and Bassett, 1974) using Inconel 750X (International Nickel Company, Inc.) gaskets and water + glycerin (crystal 1 and iron spinel) or 4:1 methanol-ethanol (crystals 2 and 3) as the fluid-pressure medium. Ruby crystals less than 10 μm maximum dimension were included in the mount, and pressures were calibrated using the pressure shift of the R₁ ruby line (Piermarini *et al.*, 1975). For each experiment, the pressure and unit-cell dimensions were measured, X-ray intensity data were collected, and the pressure and unit-cell dimensions were remeasured. Pressures and unit-cell dimensions measured before and after data collection agreed.

Details of procedures for crystal mounting, crystal centering on the four-circle diffractometer, and unit-cell determination are given by Finger and King (1978) and Hazen and Finger (1977a).

High-temperature techniques

Mullite wool was used to pack the crystal of Ni₂SiO₄ in an open capillary of fused silica that was mounted on an alumina ceramic rod with ground zirconia and Zircoa Bond 6 as a high-temperature adhesive. The cement was cured at 200°C for several hours; then the assembly was mounted on the single-crystal diffractometer, and the unit-cell dimensions were measured at several temperatures (Table 1) with the computer-controlled furnace described by Finger *et al.* (1973). Although all heating was done with the crystal in air, no degradation of the sample was observed.

Refinement

All sets of measured intensities included observations from several reflections related by symmetry, which were averaged before refinement. The least-squares program RFINE (Finger and Prince, 1975) was used for all refinement calculations. Neutral scattering factors (Cromer and Mann, 1968) and anomalous scattering coefficients (Cromer and Liber-

Table 1. Refinement conditions, refined parameters, and selected distances and angles for silicate spinels

| | Ni ₂ SiO ₄ | | | | | | | | Fe ₂ SiO ₄ |
|--|----------------------------------|-----------|-----------|-----------|-----------|-----------|-----------|-----------|----------------------------------|
| | 0.001 | 0.001* | 0.001 | 11.2(5) | 22.5(5) | 31.0(5) | 36.5(5) | 38.2(5) | 0.001 |
| P (kbar) | 0.001 | 0.001* | 0.001 | 11.2(5) | 22.5(5) | 31.0(5) | 36.5(5) | 38.2(5) | 0.001 |
| T (°C) | 23 | 23 | 700(10) | 23 | 23 | 23 | 23 | 23 | 23 |
| No. of reflections | 129 | 131 | 66 | 38 | 58 | 57 | 63 | 38 | 138 |
| No. of observations** | 112 | 111 | 58 | 32 | 49 | 48 | 47 | 32 | 121 |
| R*** all data | 2.4 | 4.6 | 2.9 | 4.9 | 4.5 | 5.0 | 6.3 | 5.1 | 1.9 |
| wR† all data | 1.5 | 2.0 | 1.9 | 2.1 | 2.2 | 2.5 | 2.6 | 2.6 | 1.4 |
| R observed | 1.5 | 2.9 | 2.0 | 3.3 | 2.3 | 2.7 | 3.0 | 4.0 | 1.5 |
| wR observed | 1.4 | 1.9 | 1.8 | 1.9 | 1.8 | 1.9 | 2.2 | 2.4 | 1.3 |
| Oxygen u | 0.2439(1)†† | 0.2441(2) | 0.2435(2) | 0.2440(4) | 0.2441(3) | 0.2442(3) | 0.2445(4) | 0.2450(6) | 0.2409(1) |
| Extinction parameter, cm (×10 ³) | 2.04(8) | 0.77(5) | 0.107(7) | 0.2440(4) | 1.6(2) | 1.8(2) | 1.6(2) | 1.6(3) | 0.05(2) |
| B _M (Å ²) | 0.25(1) | 0.30(1) | 1.14(3) | 0.54(6) | 0.43(4) | 0.39(3) | 0.45(4) | 0.51(7) | 0.40(1) |
| B _{Si} | 0.20(1) | 0.23(2) | 0.87(4) | 0.44(9) | 0.39(6) | 0.26(6) | 0.35(8) | 0.53(12) | 0.27(1) |
| B _O | 0.34(1) | 0.45(5) | 1.21(5) | 0.65(10) | 0.42(6) | 0.45(6) | 0.48(7) | 0.78(11) | 0.41(1) |
| Si-O (Å) | 1.657(1) | 1.660(3) | 1.661(1) | 1.651(6) | 1.654(4) | 1.653(4) | 1.657(6) | 1.664(8) | 1.654(1) |
| O-O (IV) | 2.705(2) | 2.710(4) | 2.713(6) | 2.696(11) | 2.697(6) | 2.699(7) | 2.705(10) | 2.712(13) | 2.701(2) |
| M-O | 2.061(1) | 2.060(2) | 2.078(2) | 2.059(4) | 2.054(2) | 2.050(3) | 2.046(4) | 2.041(5) | 2.136(1) |
| O-O (shared) | 2.983(2) | 2.978(4) | 3.011(6) | 2.982(11) | 2.972(6) | 2.964(7) | 2.954(10) | 2.941(13) | 3.123(2) |
| O-O (unshared) | 2.846(1) | 2.846(1) | 2.864(1) | 2.841(1) | 2.836(1) | 2.833(1) | 2.831(1) | 2.830(1) | 2.916(1) |
| O-M-O (°) | 92.69(5) | 92.60(8) | 92.87(10) | 92.8(2) | 92.7(1) | 92.6(1) | 92.4(2) | 92.2(2) | 93.93(4) |
| O-M-O (°) | 87.31(5) | 87.40(8) | 87.13(10) | 87.2(2) | 87.3(1) | 87.4(1) | 87.6(2) | 87.8(2) | 86.07(4) |

*Data collected at the Smithsonian Institution.

**I > 2σ.

***R = Σ||F_o| - |F_c||/Σ|F_o|.†Weighted R = [Σw(|F_o| - |F_c|)²/ΣwF_o²]^{1/2}.

††Parenthesized figures represent esd's of least units cited.

man, 1970) were used for all atoms. An isotropic extinction parameter (Zachariassen, 1968) was included in all refinements. The high-pressure refinements also included use of the "robust/resistant" techniques described by Prince and Nicholson (1978). These calculations are relatively insensitive to large systematic errors in the measured structure factors. Table 1 lists the number of independent observed reflections² ($I > 2\sigma$), residuals, and unit-cell parameters for the various experimental conditions. The room pressure and temperature results include one set of data measured at the Geophysical Laboratory and an additional data set measured at the Smithsonian Institution. No systematic differences are observed.

Previous workers (Yagi *et al.*, 1974; Marumo *et al.*, 1974, 1977; Morimoto *et al.*, 1974) have found a slight disorder between the Si and R²⁺ positions, so an occupancy factor, subject to a constraint of constant chemical composition, was refined for the data collected under room conditions. It differed so little from zero that complete cation ordering was assumed for all further calculations.

Anisotropic temperature factors were refined for all data sets. The ellipsoid for oxygen is constrained to be uniaxial with the unique axis along [111]. At

room pressure the ellipsoid is an oblate spheroid. For two of the high-pressure refinements, at 11.2 and 36.5 kbar, the ellipsoid is compressed along [111] to the point that the thermal parameters are nonpositive definite, indicating uncorrected systematic errors in the data. None of the high-pressure refinements were significantly improved by refinement of anisotropic parameters. Results with isotropic thermal factors are presented in Table 1.

Results

Compression of silicate spinels

Unit-cell parameters of nickel and iron silicate spinels at several pressures are listed in Table 2. Unit cells are refined as triclinic to detect strain resulting from nonhydrostatic conditions. All cells are cubic within three estimated standard deviations except for Ni₂SiO₄ crystal 1 in glycerin plus water at 55 kbar. Previously reported data on γ-Ni₂SiO₄ at this pressure (Finger *et al.*, 1977) are probably in error because of nonhydrostatic stress.

The bulk moduli for these spinels have been obtained from second-order Birch-Murnaghan equations of state. In the calculations, it was not possible to obtain a meaningful refinement of the variation of bulk modulus with pressure [the pressure derivative of the bulk modulus (K') became very large]. Thus the value of K' was fixed at 4.0, which is equivalent

² Tables of observed and calculated structure factors are available from the authors.

Table 2. Unit-cell parameters for silicate spinels at several pressures*

| P (kbar) | Crystal No. | a ₁ (Å) | a ₂ (Å) | a ₃ (Å) | α ₁ (°) | α ₂ (°) | α ₃ (°) | v (Å ³) | \bar{a} (Å) |
|--------------------------------------|-------------|--------------------|--------------------|--------------------|--------------------|--------------------|--------------------|---------------------|---------------|
| Ni₂SiO₄ | | | | | | | | | |
| 0.001 | 1 | 8.0445(10)** | 8.0444(9) | 8.0438(8) | 89.996(8) | 89.995(9) | 90.000(9) | 520.5(1) | 8.0442 |
| 20(1) | 1 | 8.0166(8) | 8.0178(8) | 8.0187(9) | 90.007(13) | 90.003(12) | 89.988(8) | 515.38(9) | 8.0175 |
| 29(1) | 1 | 8.012(4) | 8.008(5) | 8.013(3) | 89.93(4) | 90.03(4) | 89.92(5) | 514.1(5) | 8.011 |
| 55(1)*** | 1 | 7.990(1) | 7.974(3) | 7.989(4) | 89.99(4) | 89.91(3) | 89.96(2) | 509.0(3) | 7.984 |
| 22.5(5) | 2 | 8.0169(5) | 8.0173(4) | 8.0169(2) | 90.004(4) | 89.996(4) | 90.012(4) | 515.28(4) | 8.0170 |
| 31.0(5) | 2 | 8.0082(5) | 8.0092(4) | 8.0086(2) | 89.999(3) | 89.999(3) | 90.009(4) | 513.66(4) | 8.0086 |
| 36.5(5) | 2 | 8.0032(7) | 8.0043(4) | 8.0032(2) | 89.999(3) | 89.998(3) | 90.011(6) | 512.68(5) | 8.0036 |
| 11.2(5) | 3 | 8.0305(6) | 8.0296(8) | 8.0304(4) | 90.008(8) | 90.003(5) | 89.998(2) | 517.82(7) | 8.0302 |
| 30.0(5) | 3 | 8.0094(2) | 8.0096(2) | 8.0097(5) | 90.003(5) | 90.005(4) | 90.005(2) | 513.84(4) | 8.0096 |
| 38.2(5) | 3 | 8.0034(8) | 8.0006(9) | 8.0001(4) | 90.02(2) | 90.03(2) | 90.01(1) | 512.3(1) | 8.0014 |
| Fe₂SiO₄ | | | | | | | | | |
| 0.001 | 1 | 8.238(2) | 8.235(2) | 8.236(2) | 90.01(2) | 90.01(2) | 89.98(2) | 558.7(2) | 8.236 |
| 20(1) | 1 | 8.207(4) | 8.215(9) | 8.211(4) | 89.97(7) | 89.97(4) | 90.09(7) | 553.5(7) | 8.211 |
| 40(1) | 1 | 8.180(3) | 8.184(11) | 8.180(3) | 89.97(6) | 90.00(3) | 90.03(6) | 547.7(8) | 8.181 |

*Unit cell refined as triclinic.

**Parenthesized figures represent esd's of least units cited.

***Nonhydrostatic pressure.

to the first-order Birch–Murnaghan equation. The bulk modulus of nickel spinel is 2.27(4) Mbar, excluding the 55 kbar (nonhydrostatic) result. For iron silicate spinel a value of 1.96(6) Mbar was obtained. Sato (1977) studied the compression of silicate spinels with powder X-ray diffraction techniques, using 4:1 methanol–ethanol as a pressure-transmitting medium. Her results for a first-order Birch–Murnaghan equation are 2.23(2) and 1.97(2) Mbar for nickel and iron spinels, respectively.

γ -Ni₂SiO₄ at high temperature

The lattice parameters of γ -Ni₂SiO₄ at seven temperatures between 23° and 700°C are recorded in Table 3. Expansion is linear within experimental error over this range,

$$a = 8.041 + 0.000078 T (^{\circ}\text{C})$$

and the thermal expansion coefficient is $9.7 \times 10^{-6} \text{ }^{\circ}\text{C}^{-1}$.

The u positional parameter of oxygen decreases by two estimated standard deviations between 23° ($u = 0.2440 \pm 0.0001$) and 700°C ($u = 0.2435 \pm 0.0002$), as recorded in Table 1. The Si–O distance remains constant at approximately 1.66Å, and the Ni–O bond expands from 2.060 to 2.078Å. Nickel silicate spinel thus responds to temperature like most other silicates, with little change in the tetrahedron but significant expansion of divalent cation polyhedra.

Structure of γ -Ni₂SiO₄ at high pressure

Deviations of the unit-cell angles from values required by symmetry are a sensitive indicator of non-

hydrostatic conditions (Finger and Hazen, 1978). The preliminary data on iron and nickel spinels (Finger *et al.*, 1977) are affected by this problem; therefore, data on γ -Ni₂SiO₄ were re-collected on two crystals at five pressures, using the modified procedures of King and Finger (1979) and Hazen and Finger (1977a). Refined parameters and selected interatomic distances and angles are listed in Table 1.

The positional parameters of oxygen obtained at various pressures are presented in Figure 1. Some nonlinear variation is evident in this diagram; however, weighted regression analysis with second-order parameters does not yield a significant improvement. The hypothesis that u is invariant throughout the metastable range ($P < 23$ kbar, Akimoto *et al.*, 1965) and increases above this pressure has also been rejected, as the data of Sato (1977) do not show any anomalous variation in the compression of nickel spinel as this pressure boundary is crossed. For the

Table 3. Unit-cell parameters for γ -Ni₂SiO₄ at several temperatures

| T (°C) | a (Å) | v (Å ³) |
|---------|-----------|---------------------|
| 23 | 8.044(1)* | 520.5(1) |
| 200(10) | 8.056(2) | 522.8(2) |
| 300(10) | 8.064(2) | 524.3(2) |
| 400(10) | 8.071(2) | 525.8(2) |
| 500(10) | 8.079(2) | 527.3(2) |
| 600(10) | 8.088(2) | 529.0(3) |
| 700(10) | 8.095(2) | 530.5(3) |

*Parenthesized figures represent esd's of least units cited.

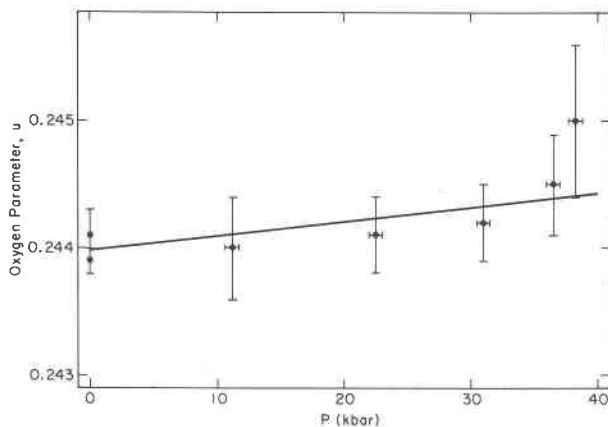


Fig. 1. The oxygen positional parameter, u , of γ - Ni_2SiO_4 vs. pressure. Weighted regression analysis was used to derive the line.

linear model, contrary to preliminary conclusions (Finger *et al.*, 1977), the ratio of octahedral to tetrahedral M–O distance, d_o/d_t , decreases with increased pressure. Between 1 atm and 38.2 kbar the Si–O distance is constant at 1.66Å (within experimental error), whereas the Ni–O distance decreases (by at least five standard deviations) from 2.06 to 2.04Å.

Electron density calculations

Difference electron density maps produced from the intensities measured in this study are similar to those previously reported by Marumo *et al.* (1974, 1977). The major features (Fig. 2a) occur approximately 0.5Å from the Ni position. Anomalies of -1.0

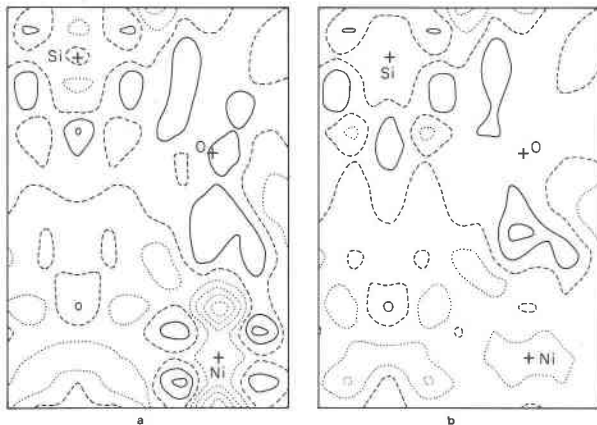


Fig. 2. Partial section of the difference electron density for γ - Ni_2SiO_4 through the plane $y = x$. Contours are at intervals of $0.2 \text{ e}/\text{Å}^3$ with the zero contour dashed and negative values dotted. Part (a) is for an anisotropic refinement and (b) is for a model with anharmonic terms for nickel. Atomic positions are labeled.

$\text{e}/\text{Å}^3$ are located along the Ni–O bond direction. Features of approximately $+0.5 \text{ e}/\text{Å}^3$ occur along $[111]$ and $[\bar{1}\bar{1}\bar{1}]$, in the openings between oxygen bonds. Although these features are not large, they are highly significant because of the low residual (1.4 percent) for the refined data set. As described by Marumo *et al.* (1974), the observed pattern of electron density could arise from the effects of the ligand fields on the $3d$ electrons of the Ni ions or from anharmonic thermal motion. In the present study, the cumulant expansion of the temperature factor (Johnson, 1970) was used to include anharmonic contributions. In the mathematical formalism employed, an expansion of the structure factor equation to fourth order in terms of products of the Miller indices is performed. The ordinary positional parameters and anisotropic thermal coefficients roughly correspond to the first- and second-order terms, respectively. For the site symmetry ($\bar{3}m$) of Ni in spinel, all odd-order terms vanish, leaving two second-order terms and four fourth-order coefficients. The fourth-cumulant terms correspond to a correction for the statistical descriptor called kurtosis or peakedness.

When the fourth-cumulant terms were included in the least-squares refinement, the weighted residual decreased from 1.4 to 1.1 percent, yielding a ratio of the weighted R factors of 1.25, whereas the R -factor-ratio test of Hamilton (1965) requires only a ratio of 1.08 to justify the additional parameters at the 0.5 percent significance level. A difference electron density map computed with the new thermal parameters is shown in Figure 2b. The anomalies in the vicinity of Ni are essentially eliminated, and the residual electron densities at the positions of oxygen and silicon are reduced. A positive residual between Ni and O is enhanced. Table 4 lists the refined thermal parameters for the ordinary and fourth-cumulant refinement. Only the d_{1111} term is significantly different from zero, and this term flattens the calculated electron density along the Ni–O bond ($[100]$). Note that the b_{ij} terms are reduced for all atoms when anharmonic terms for Ni are introduced. Although the expansion of the fourth-order terms for Ni has significantly reduced the R factor and virtually eliminated the residuals in the difference electron density, it is impossible to distinguish, from the X-ray data, between a static distortion of the electron distribution and nonharmonic vibrations. Studies of the structure with inelastic neutron scattering techniques could resolve this question.

The fourth-cumulant formalism was also applied

Table 4. Thermal parameters* for γ -Ni₂SiO₄

| Atom | Parameter | Refined value ($\times 10^5$) | |
|------|-------------|---------------------------------|-----------------------|
| | | Ordinary refinement | Anharmonic refinement |
| Ni | b_{11} ** | 96(3)† | 78(8) |
| | b_{12} | -5(4) | -4(2) |
| | d_{1111} | - | -0.16(3) |
| | d_{1112} | - | -0.00(1) |
| | d_{1122} | - | 0.02(1) |
| | d_{1123} | - | 0.00(1) |
| Si | b_{11} | 76(5) | 67(5) |
| O | b_{11} | 130(6) | 122(5) |
| | b_{12} | -15(10) | -12(8) |

*Thermal parameters are of the form:

$$\exp\left[-\sum_j \sum_k h_j h_k b_{jk} - \sum_j \sum_k \sum_l \sum_m h_j h_k h_l h_m d_{jklm}\right]$$

**Symmetry constraints for atoms are as follows:

$$\text{Ni: } b_{11} = b_{22} = b_{33}, b_{12} = b_{13} = b_{23}, d_{1111} = d_{2222} = d_{3333}, \\ d_{1123} = d_{1223} = d_{1233}, d_{1112} = d_{1113} = d_{1222} = d_{1333} = \\ d_{2333}, d_{1122} = d_{1133} = d_{2233}$$

$$\text{Si: } b_{11} = b_{22} = b_{33}, b_{12} = b_{13} = b_{23} = 0$$

$$\text{O: } b_{11} = b_{22} = b_{33}, b_{12} = b_{13} = b_{23}$$

†Parenthesized figures represent $\text{esd}'s$ of least units cited.

to the iron spinel data. The difference electron densities after ordinary refinement (Fig. 3a) showed features of $-0.6 \text{ e}/\text{A}^3$ along [111] and positive residuals of $0.6 \text{ e}/\text{A}^3$ along the Fe-O bond. The topology of the electron density residuals in the vicinity of iron is similar to the results of Marumo *et al.* (1977); however, there is a reversal in sign. After refinement of the fourth-cumulant terms (Fig. 3b), both types of anomalies were reduced in height and areal extent,

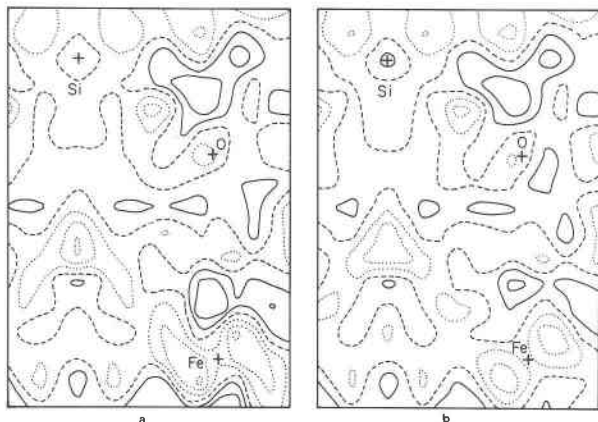


Fig. 3. Partial section of the difference electron density for γ -Fe₂SiO₄ through the plane $y = x$. See legend of Fig. 2.

but the reduction in weighted R was not sufficient to justify the additional parameters in the refinement.

Discussion

Unit-cell a vs. oxygen u

A significant result of this study is that the relationship between unit-cell edge a and oxygen parameter u (Fig. 4) is essentially linear. This relationship holds for Co₂SiO₄, Fe₂SiO₄, and Ni₂SiO₄ at several pressures and temperatures, and is, therefore, independent of temperature, pressure, and octahedral composition for the transition metal silicate spinels. In addition, all points of Figure 4 are close to the line of constant Si-O distance of 1.66 Å. Silicate spinels in the range of P , T , and X studied, consequently, appear to have a constant tetrahedral volume of $2.34(2)\text{A}^3$ (Table 5), whereas the size of the M-O octahedron is the principal structural variable.

Polyhedral bulk moduli of γ -Ni₂SiO₄

Polyhedral volumes of Si-O tetrahedra and Ni-O octahedra for nickel silicate spinel are listed in Table 5. As noted above, there is no systematic change with pressure in the tetrahedral volume, and the bulk modulus for that polyhedron is greater than 2.5 Mbar. A number of other silicates have tetrahedral bulk moduli of 2.5 ± 0.5 Mbar (Hazen and Finger, 1977a).

The Ni-O octahedron has a calculated bulk modulus of 1.7(1) Mbar, based on weighted linear regression of data in Table 5. This value is somewhat less

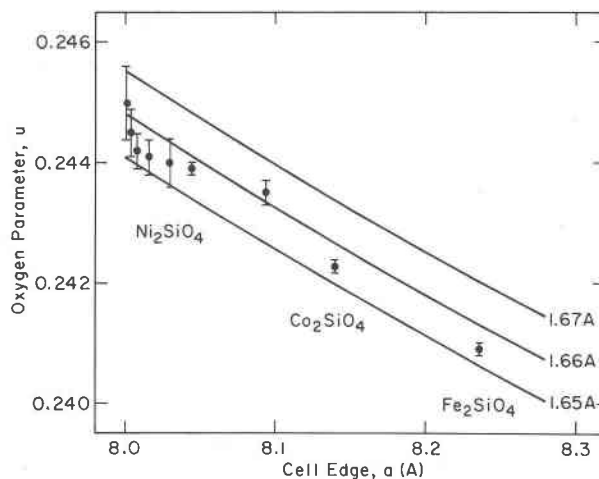


Fig. 4. The oxygen positional parameter, u , of several silicate spinels vs. the unit-cell edge, a . Calculated lines corresponding to constant Si-O distances of 1.65, 1.66, and 1.67 Å are shown.

Table 5. Polyhedral volumes for γ -Ni₂SiO₄

| T (°C) | P (kbar) | V_{Si} (Å ³) | V_{Ni} (Å ³) |
|----------|------------|----------------------------|----------------------------|
| 23 | 0.001 | 2.335 | 11.63 |
| 23* | 0.001 | 2.348 | 11.62 |
| 23 | 11.2 | 2.327 | 11.57 |
| 23 | 22.5 | 2.322 | 11.50 |
| 23 | 31.0 | 2.331 | 11.42 |
| 23 | 36.5 | 2.340 | 11.37 |
| 23 | 38.2 | 2.361 | 11.30 |
| 700 | 0.001 | 2.352 | 11.92 |

*Data collected at the Smithsonian Institution.

than the value of 1.95(5) Mbar reported by Bassett and Takahashi (1974) for NiO. Hazen and Finger (1977a) proposed an inverse relationship between polyhedral bulk modulus, K , and polyhedral volume, V , for divalent cation polyhedra: $K = 21/V$ Mbar. The predicted value for the Ni-O octahedron with V of 11.6Å³ is 1.8 Mbar, which is consistent with the observed value.

The olivine/spinel transition

At room temperature the transformation of iron and nickel olivine to the spinel form takes place at 35 and 23 kbar, respectively (Akimoto *et al.*, 1965, 1976, 1977). From compressibility data for spinels from the present study, combined with observed (Hazen, 1977) and predicted (Hazen and Finger, 1977b) values of olivine and iron spinel polyhedral compressibilities, a comparison of olivine and spinel structures at the transition pressure can be made. From these calculations, it appears that the ratio of octahedral to tetrahedral distance, d_o/d_t , decreases in both olivines and spinels with increasing pressure or decreasing temperature. For Ni₂SiO₄ at 23 kbar, d_o/d_t is 1.27 and 1.23 for olivine and spinel, respectively. For Fe₂SiO₄ at 35 kbar, the equivalent quantities are 1.32 and 1.28. As Kamb (1968) noted, there is a sizable reduction in d_o/d_t as the structure changes from olivine to spinel. The ratio at transition is not independent of composition, nor are values of d_o/d_t constant along the pressure-temperature range of the transition for a given composition. For example, at 1000°C and 35 kbar, also on the $\alpha \rightleftharpoons \gamma$ transition curve for Ni₂SiO₄ (Akimoto *et al.*, 1976), d_o/d_t is predicted to be 1.29 and 1.25 for olivine and spinel, respectively. Although this ratio is altered in the olivine-spinel transition, it is obviously an oversimplification, as noted by Kamb, to define the stability limits of spinel in terms of a single parameter.

Acknowledgments

The authors thank Dr. Daniel Appleman of the Smithsonian Institution for the use of his diffractometer system and Drs. Peter M. Bell and H. K. Mao, Geophysical Laboratory, for the use of their pressure calibration equipment. Drs. Felix Chayes and Gordon Davis suggested valuable changes in the manuscript. Partial financial support for this study was provided by NSF grant EAR77-23171.

References

- Akimoto, S., H. Fujisawa and T. Katsura (1965) The olivine-spinel transition in Fe₂SiO₄ and Ni₂SiO₄. *J. Geophys. Res.*, **70**, 1969-1977.
- , Y. Matsui and Y. Syono (1976) High-pressure crystal chemistry of orthosilicates and the formation of the mantle transition zone. In R. G. J. Strens, Ed., *The Physics and Chemistry of Minerals and Rocks*, p. 327-363. Wiley, New York.
- , T. Yagi and K. Inoue (1977) High temperature-pressure phase boundaries in silicate systems using in situ x-ray diffraction. In M. H. Manghnani and S. Akimoto, Eds., *High-Pressure Research*, p. 585-602. Academic Press, New York.
- Bassett, W. A. and T. Takahashi (1974) X-ray diffraction studies up to 300 kbar. *Advances in High-Pressure Research*, **4**, 165-247.
- Cromer, D. T. and D. Liberman (1970) Relativistic calculations of anomalous scattering factors for X-rays. *J. Chem. Phys.*, **53**, 1891-1898.
- and J. B. Mann (1968) X-ray scattering factors computed from numerical Hartree-Fock wave functions. *Acta Crystallogr.*, **A34**, 321-324.
- Finger, L. W. and R. M. Hazen (1978) Crystal structure and compression of ruby to 46 kbar. *J. Appl. Phys.*, **49**, 5823-5826.
- and H. E. King (1978) A revised method of operation of the single-crystal diamond cell and the refinement of the structure of NaCl at 32 kbar. *Am. Mineral.*, **63**, 337-342.
- and E. Prince (1975) A system of Fortran IV computer programs for crystal structure calculations. *Natl. Bur. Stand. (U.S.) Tech. Note 854*.
- , C. G. Hadidiacos and Y. Ohashi (1973) A computer-automated, single-crystal, X-ray diffractometer. *Carnegie Inst. Wash. Year Book*, **72**, 694-699.
- , R. M. Hazen and T. Yagi (1977) High-pressure crystal structures of the spinel polymorphs of Fe₂SiO₄ and Ni₂SiO₄. *Carnegie Inst. Wash. Year Book*, **76**, 504-505.
- Hamilton, W. C. (1965) Significance tests on the crystallographic R factor. *Acta Crystallogr.*, **18**, 502-510.
- Hazen, R. M. (1977) Effects of temperature and pressure on the crystal structure of ferromagnesian olivine. *Am. Mineral.*, **62**, 286-295.
- and L. W. Finger (1977a) Modifications in high-pressure, single-crystal diamond-cell techniques. *Carnegie Inst. Wash. Year Book*, **76**, 655-656.
- and ——— (1977b) Compression models for oxides and silicates (abstr.). *Geol. Soc. Am. Abstracts with Programs*, **9**, 1008-1009.
- Johnson, C. K. (1970) Generalized treatments for thermal motion. In B. T. M. Willis, Ed., *Thermal Neutron Diffraction*, p. 132-160. Oxford University Press, London.
- Kamb, B. (1968) Structural basis of the olivine-spinel relation. *Am. Mineral.*, **53**, 1439-1455.

- King, H. E. and L. W. Finger (1979) Diffracted beam crystal centering and its application to high-pressure crystallography. *J. Appl. Crystallogr.*, in press.
- Marumo, F., M. Isobe and S. Akimoto (1977) Electron-density distributions in crystals of γ -Fe₂SiO₄ and γ -Co₂SiO₄. *Acta Crystallogr.*, B33, 713–716.
- , ——, Y. Saito, T. Yagi and S. Akimoto (1974) Electron-density distribution in crystals of γ -Ni₂SiO₄. *Acta Crystallogr.*, B30, 1904–1906.
- Merrill, L. and W. Bassett (1974) Miniature diamond anvil pressure cell for single crystal X-ray diffraction studies. *Rev. Sci. Instrum.*, 45, 290–294.
- Morimoto, N., M. Tokonami, M. Watanabe and K. Koto (1974) Crystal structures of three polymorphs of Co₂SiO₄. *Am. Mineral.*, 59, 475–485.
- Piermarini, G. J., S. Block, J. D. Barnett and R. A. Forman (1975) Calibration of the pressure dependence of the *R* ruby fluorescence line to 195 kbar. *J. Appl. Phys.*, 46, 2774–2780.
- Prince, E. and W. L. Nicholson (1978) A test of robust/resistant refinement on synthetic data sets (abstr.). *Program and Abstracts, Am. Crystallogr. Assoc.*, 6, 37.
- Ringwood, A. E. (1958a) The constitution of the mantle III: consequences of the olivine–spinel transition. *Geochim. Cosmochim. Acta*, 15, 195–212.
- (1958b) Olivine–spinel transition in fayalite. *Bull. Geol. Soc. Am.*, 69, 129–130.
- Sato, Y. (1977) Equation of state of mantle minerals determined through high-pressure X-ray study. In M. H. Manghnani and S. Akimoto, Eds., *High-Pressure Research*, p. 307–324. Academic Press, New York.
- Smyth, J. R. (1975) High-temperature crystal chemistry of fayalite. *Am. Mineral.*, 60, 1092–1097.
- and R. M. Hazen (1973) The crystal structures of forsterite and hortonolite at several temperatures up to 900°C. *Am. Mineral.*, 58, 588–593.
- Syono, Y., M. Tokonami and Y. Matsui (1971) Crystal field effect on the olivine–spinel transformation. *Phys. Earth Planet. Interiors*, 4, 347–352.
- Wyllie, P. J. (1970) *The Dynamic Earth*. Wiley, New York.
- Yagi, T., F. Marumo and S. Akimoto (1974) Crystal structures of spinel polymorphs of Fe₂SiO₄ and Ni₂SiO₄. *Am. Mineral.*, 59, 486–490.
- Zachariasen, W. H. (1968) Experimental tests of the general formula for the integrated intensity of a real crystal. *Acta Crystallogr.*, A24, 212–216.

*Manuscript received, January 15, 1979;
accepted for publication, May 7, 1979.*